Preparation of graphene/aligned carbon nanotube array composite films for thermal packaging applications

Japanese Journal of Applied Physics

REGULAR PAPER

Preparation of graphene/aligned carbon nanotube array composite films for thermal packaging applications

Japanese Journal of Applied Physics **58**, SHHH01 (2019) **REGULAR PAPER**
https://doi.org/**10.7567/1347-4065/ab1bd0**

Preparation of graphene/aligned carbon nanotube array composite films for thermal packaging applications

Bo Shan[1], Guangjie Yuan[1*], Haohao Li[1], and Johan Liu[1,2*]

[1]*SMIT Center, School of Automation and Mechanical Engineering, Shanghai University, Shanghai 201800, People's Republic of China*
[2]*Electronics Materials and Systems Laboratory, Department of Microtechnology and Nanoscience (MC2), Chalmers University of Technology, SE-412 96 Göteborg, Sweden*

[*]E-mail: guangjie@shu.edu.cn; jliu@chalmers.se

Received December 6, 2018; accepted April 14, 2019; published online June 26, 2019

Vertically aligned carbon nanotube arrays (VACNTs) have been successfully achieved by CVD. The carbon nanotubes were almost triple-walled. Furthermore, the graphene/VACNT composite films have been prepared as thermal interface materials, using photolithographic and densification processes. Compared with pure epoxy resin, the longitudinal thermal conductivity of the composite films was obviously improved, which confirmed that VACNTs provided additional longitudinal heat transfer channels in the films. Furthermore, their longitudinal thermal conductivity was largely dependent on the distribution of VACNTs. The transversal thermal conductivity of the composite film with a pattern size of 300 μm was about seven times higher than that of pure epoxy resin. This indicated that graphene provided additional horizontal heat transfer channels to achieve the enhancement of transversal thermal conductivity in composite films.

1. Introduction

With the development of high-power electronic products, more heat generates in chip. Furthermore, non-uniform heat dissipation also leads to the overheating of specific areas in chip, largely affecting the computing performance and reliability of electronic devices. Generally, if the temperature of the hot spot is reduced by 20 °C, the lifetime of transistors would be extended by one order of magnitude.[1–5)] In the real chip packaging structure, the actual contact is greatly restricted by the rough surface among heat sink, heat spreader and chip.[6–8)] They only have 1%–2% physical contact with each other, while the other space is filled with air in the gaps. To overcome this problem, thermal interface materials (TIMs) have been widely used to fill the rough contact surfaces.[9–13)]

Recently, carbon nanotube (CNT) has attracted wide attention in the heat dissipation of electronic packaging. The experimental thermal conductivity of multi-wall carbon nanotube or single-wall carbon nanotube is more than 3000 $Wm^{-1}K^{-1}$ at RT.[14,15)] Furthermore, the vertically aligned carbon nanotube arrays (VACNTs) have good alignment, high surface area, high carbon purity, and excellent electrical and thermal conductivities, which have been shown to be advantageous for thermal dissipation applications.[16–19)] Recently, some VACNT/polymer composite films have been reported as TIMs. Reference 20 reported the superiority of VACNTs versus randomly dispersed CNTs in S160 elastomer matrix. After VACNTs were combined with the matrix, the axial thermal conductivity of the composite was three times higher than that of the matrix.[20)] Reference 21 also reported the longitudinal thermal conductivity of the composite of epoxy resin and VACNTs was apparently improved along the axis, and its thermal conductivity increased to be more than 1.8 $Wm^{-1}K^{-1}$ at 30 °C. Reference 22 revealed that the longitudinal thermal conductivity of the composite of poly-dimethyl siloxane (PDMS) and VACNTs was much larger than that of the polymer matrix. However, it was also found that its transverse thermal conductivity was 2–4 times smaller than its longitudinal thermal conductivity.[22)] In a word, VACNTs could largely increase the longitudinal thermal conductivity of composite films, but their transverse thermal conductivity was still low, due to the good alignment of the VACNTs.

Graphene has many outstanding properties, such as high electronic mobility, good mechanical properties, excellent thermal conductivity and thermal stability.[23)] Its in-plane thermal conductivity was found to be about 5300 $Wm^{-1}K^{-1}$ at RT.[24–26)] Therefore, we plan to develop a composite film as the TIM, based on VACNTs, graphene and epoxy resin. To achieve the enhancement of longitudinal and transversal thermal conductivities at the same time, graphene was used to provide additional horizontal heat transfer pathways, and VACNTs were used to offer additional vertical heat transfer channels in the composite films.

2. Experimental methods

Epoxy resin (N,N-Diglycidyl-4-glycidyloxyaniline, $C_{15}H_{19}NO_4$) was purchased from Sigma-Aldrich Trading Co., Ltd. A curing agent (1-(2-Cyanoethyl)-2-ethyl-4-methylimidazole (contains 5-methyl isomer), $C_9H_{13}N_3$) and diluent [ethylene glycol diglycidyl ether (mixture)] were purchased from TCI Chemical Industrial Development Co., Ltd. An Al_2O_3 layer (20 nm thickness) was deposited on Si substrates first. An Fe layer (1 nm thickness) was subsequently deposited on the Al_2O_3 layer as the catalyst for synthesizing the VACNTs. Graphene was purchased from Nanjing XFNANO Materials Tech Co., Ltd. Its planar size was about 5 μm and its thickness was 1 $\sim$ 5 nm. Figure 1 shows the preparation process for the graphene/VACNT composite film. First, the photolithographic process was used to pattern the catalyst on Al_2O_3/Si substrates using a lithography machine (URE-2000S/A). The pattern sizes were 200, 300, 400, 500 and 600 μm, and the distance was 150 μm among the patterns. After patterning, the region for the growth of VACNTs accounted for 25.6%, 34.9%, 41.5%, 46.5% and 50.3% in the whole area, respectively. Second, VACNTs were deposited by CVD (AIXTRON Black Magic II) at the growth temperature of 650 °C, and the deposition time was 0.5 h. Before the growth of VACNTs, the catalyst was annealed at a temperature of 550 °C. The annealing period was 180 s and hydrogen (H_2) was supplied. After that, acetylene (C_2H_2) and

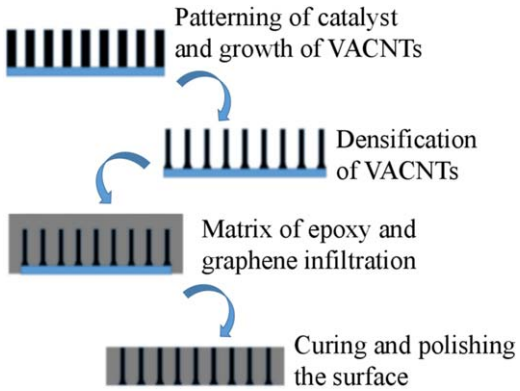

Fig. 1. (Color online) Schematics of the preparation process for the graphene/VACNT composite film.

H_2 were introduced into the reaction chamber as the carbon source gas and reducing gas, respectively. Third, VACNTs were densified by the acetone vapor method and the period was 20 s. Fourth, graphene, epoxy resin, curing agent and diluent were mixed as the matrix. The epoxy mixture included epoxy resin, curing agent and diluents, and their mass ratio was 7.5:0.5:2. The graphene was mixed with the epoxy mixture to make the matrix, of which graphene comprised 10%. After that, VACNTs were immersed into the matrix and cured in the oven at 150 °C for 2 h. Finally, the composite film was peeled off from the Si substrate and polished to about 400 μm. The tips of the VACNTs should be protruded from both surfaces of the composite film.

The cross-sections of VACNTs and composite films were characterized by field-emission scanning electron microscopy (Merlin Compact). The morphology of the VACNTs was analyzed by transmission electron microscopy (TEM, Tecnai G2 F20 S-TWIN). Raman spectra of the VACNTs were recorded by inVia Reflex, using a laser excitation wavelength of 632.8 nm. The thermal diffusivity (α) of the composite films was tested by a laser flash thermal analyzer (Netzach LFA 447) at RT. The sample sizes were φ 12.7 and 25.4 mm for the analysis of longitudinal and transverse thermal diffusivities, as the sample carrier was standard with fixed size. The samples were first heated by light pulses and then the temperature rise at three different positions was measured by an infrared detector. The thermal diffusivity (α) of the composite films was determined by analyzing the temperature-time curve. The thickness of the samples was about 400 μm. Their specific heat capacity (Cp) was detected by a differential scanning calorimeter (Mettler Toledo DSC1). The thermal conductivity (λ) could be calculated by Eq. (1)

$$\lambda = \alpha \times Cp \times \rho, \tag{1}$$

where ρ represents the density of the composite films, and it was measured by water displacement.

3. Results and discussion

3.1. Characterization of VACNTs

Figures 2(a) and 2(b) show that VACNTs have been successfully deposited at 650 °C, and there are actually many gaps inside them at high magnification. Due to a crowding effect, the CNTs supported each other by van der Waals attraction, which made them relatively well aligned.[27] Furthermore, their growth rate was estimated to be 0.257 μm s^{-1}. Figure 3 shows the Raman spectra of the VACNTs grown on Fe/Al_2O_3/Si substrate. Generally, G peak was near 1580 cm^{-1}, which was the symmetry vibration of the optical mode and six-ring plane expansion.[28] D peak was around 1360 cm^{-1}, which was a vibration mode and caused by the edge or defect of the microcrystal plane.[28] Furthermore, G′ peak was usually around 2700 cm^{-1}.[28,29] The ratio of I_D and I_G was calculated to be 1.45, which indicated that our prepared VACNTs were multi-walled. The morphology of the VACNTs was also analyzed by TEM, as shown in Figs. 4(a) and 4(b). Figure 4(b) shows that the VACNTs were almost triple-walled, which was consistent with the result of Raman analysis.

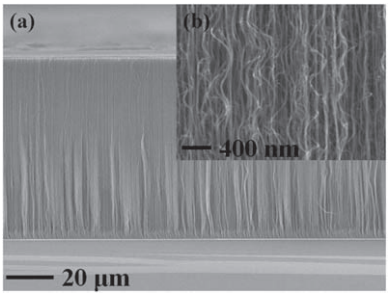

Fig. 2. Cross-section scanning electron microscope (SEM) images of VACNTs at 650 °C: (a) at low magnification; (b) at high magnification.

3.2. Preparation of composite films

As shown in Fig. 2(b), inside the VACNTs there were a lot of gaps, which were filled with air. The thermal conductivity of air was only 0.023 Wm^{-1} K^{-1} at RT, so densification of the VACNTs was used to remove it. Figures 5(a)–5(e) show that VACNTs were achieved on the patterned catalyst and the pattern size was changed from 200 to 600 μm. Figures 5(f)–5(j) show the morphology of the VACNTs after densification. As can be seen, the VACNTs collapsed after densification to a pattern size of 200 μm, which might be caused by the high aspect ratio of their features. With the pattern size from 300–500 μm, the obvious densification of VACNTs was achieved.

Figures 6(a) and 6(b) show the cross-section image of the composite film, including VACNTs and graphene. The VACNTs and matrix were well contacted, and there were almost no apparent voids in the composite film. Therefore, we could conclude that good quality graphene/VACNT composite film had been successfully synthesized.

3.3. Thermal property of composite films

Figure 7(a) shows the longitudinal thermal conductivity of graphene/VACNT composite films with different pattern

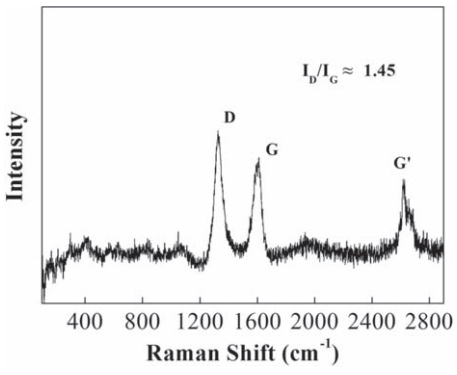

Fig. 3. Raman spectra of VACNTs grown on the Fe/Al_2O_3/Si substrate.

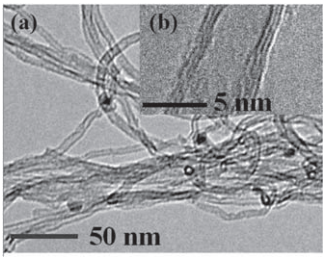

Fig. 4. TEM images of VACNTs grown on the $Fe/Al_2O_3/Si$ substrate: (a) at low magnification; (b) at high magnification.

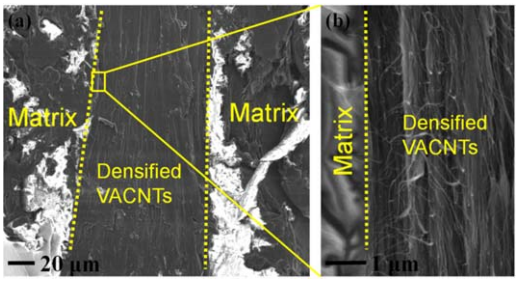

Fig. 6. (Color online) Cross-section SEM images of the graphene/VACNT composite film: (a) at low magnification; (b) at high magnification.

sizes. This shows that VACNTs could indeed enhance the longitudinal thermal conductivity of composite films, compared with pure epoxy resin and matrix. This confirmed that the VACNTs offered additional vertical heat transfer channels in the composite films. With the pattern size increasing from 300 to 600 μm, the ratio of the growth region increased from 34.9% to 50.3%. We could conclude that the longitudinal thermal conductivity of composite films decreased from 1.85 to 1.50 $Wm^{-1}K^{-1}$, when the ratio of the growth region increased and the pattern size reduced. This indicated that the improvement of the longitudinal thermal conductivity was not only dependent on the total number of VACNTs, but the distribution of VACNTs in composite films. The cluster of VACNTs grown on each patterned catalyst area could be seen as a large-diameter vertical carbon nanotube (LVCNT) and the number of these LVCNTs largely decided the longitudinal thermal conductivity of the composite films. When the pattern size reduced to 300 μm, the composite film had the highest number of LVCNTs. In addition, its longitudinal thermal conductivity was the highest, which was about nine times higher than that of pure epoxy resin.

Figure 7(b) shows the transverse thermal conductivity of the graphene/VACNT composite film with the pattern size of 300 μm, compared with the pure epoxy resin and matrix. The transverse thermal conductivity of the pure epoxy resin, matrix and composite film were measured to be about 0.22, 1.92 and 1.65 $Wm^{-1}K^{-1}$, respectively. The addition of graphene effectively increased the transverse thermal conductivity of the composite film, which was about seven times higher than that of pure epoxy resin. This confirmed that graphene offered additional horizontal heat transfer pathways in the composite film. However, compared with the matrix, the transverse thermal conductivity of the composite film was a little lower, which was caused by the low transverse thermal conductivity of VACNTs in it. Generally, the

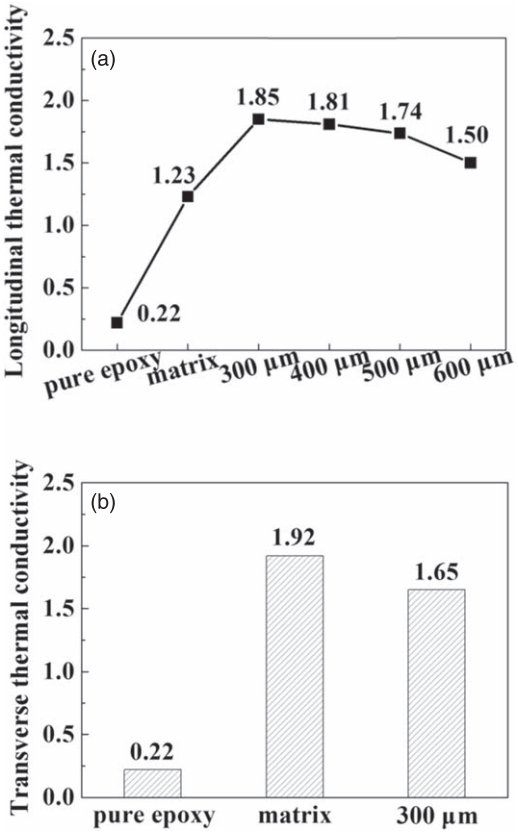

Fig. 7. Thermal property of graphene/VACNT composite films: (a) longitudinal thermal conductivity of composite films with different pattern size; (b) transverse thermal conductivity of the composite film with the pattern size of 300 μm.

transverse (radial) thermal conductivity of CNTs was much lower than their longitudinal (axial) thermal conductivity.[30] According to Figs. 7(a) and 7(b), we could also conclude that

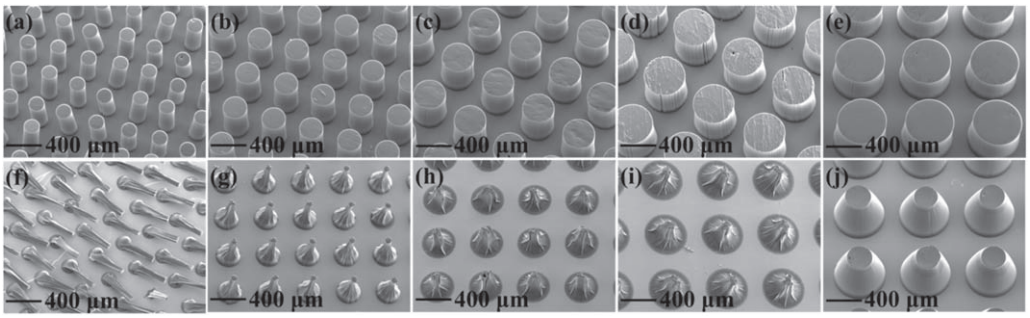

Fig. 5. SEM images of VACNTs with different pattern size: (a) 200 μm; (b) 300 μm; (c) 400 μm; (d) 500 μm; (e) 600 μm. SEM images of VACNTs after densification with different pattern size: (f) 200 μm; (g) 300 μm; (h) 400 μm; (i) 500 μm; (j) 600 μm.

the thermal conductivity of the matrix was anisotropic and its transverse thermal conductivity was higher than its longitudinal thermal conductivity. This indicated that the dispersion state of graphene was closer to horizontal alignment in the matrix and composite film.

4. Conclusions

Multilayer VACNTs were successfully deposited by CVD using C_2H_2 and H_2. After that, VACNTs were used to synthesize the composite film together with graphene and epoxy resin as the matrix. There were almost no obvious voids in the composite films, in which VACNTs and graphene were used as the additional longitudinal and transverse heat transfer pathways, respectively. Compared with pure epoxy resin, the longitudinal and transverse thermal conductivities of composite films were apparently enhanced. The longitudinal thermal conductivity of composite films was not only dependent on the total number of VACNTs, but the distribution of VACNTs in the films, which had a significant impact on the improvement of their heat dissipation performance. When the pattern size reduced to 300 μm, the longitudinal thermal conductivity of the composite film was the highest. Furthermore, the addition of graphene effectively increased the transverse thermal conductivity of the composite film, which was about 1.65 $Wm^{-1}K^{-1}$.

Acknowledgments

The authors gratefully acknowledge the financial support of the Ministry of Science and Technology of China (Contract No: 2017YFB0406000) and the Shanghai Municipal Education Commission (Shanghai University High Education Peak Discipline Program).

1) A. Ramasubramaniam, D. Naveh, and E. Towe, Nano Lett. **11**, 1070 (2010).
2) Y. Zhang, H. Han, N. Wang, P. Zhang, Y. F. Fu, M. Murugesan, M. Edwards, K. Jeppson, S. Volz, and J. Liu, Adv. Funct. Mater. **25**, 4430 (2015).
3) Z. L. Gao, Y. Zhang, Y. F. Fu, M. M. F. Yuen, and J. Liu, Carbon **61**, 342 (2013).
4) Z. Yan, G. Liu, J. M. Khan, and A. A. Balandin, Nat. Commun. **3**, 827 (2012).
5) K. M. Shahil and A. A. Balandin, Nano Lett. **12**, 861 (2012).
6) A. Yu, P. Ramesh, M. E. Itkis, E. Bekyarova, and R. C. Haddon, J. Phys. Chem. C **111**, 7565 (2007).
7) H. Im and J. Kim, Carbon **50**, 5429 (2012).
8) G. Li, J. Liu, G. Jiang, and H. Liu, Adv. Mech. Eng. **7**, 1 (2017).
9) V. Singhal, T. Siegmund, and S. V. Garimella, IEEE T. Compon. Pack. T **27**, 244 (2004).
10) C. Lin and D. D. L. Chung, Carbon **47**, 295 (2009).
11) D. D. L. Chung, J. Mater. Eng. Perform. **10**, 56 (2001).
12) R. S. Prasher, IEEE T. Compon. Pack. T **28**, 230 (2005).
13) S. Wang, Y. Cheng, R. Wang, J. Sun, and L. Gao, ACS Appl. Mater. Inter. **6**, 6481 (2014).
14) P. Kim, L. Shi, A. Majumdar, and P. L. Mceuen, Phys. Rev. Lett. **87**, 215502 (2001).
15) E. Pop, D. Mann, Q. Wang, K. Goodson, and H. Dai, Nano Lett. **6**, 96 (2006).
16) R. Cross, B. A. Cola, T. Fisher, X. Xu, K. Gall, and S. Graham, Nanotechnology **21**, 445705 (2010).
17) J. Xu and T. S. Fisher, IEEE T. Compon. Pack. T **29**, 261 (2006).
18) J. Marklin, N. Halonen, G. Toth, A. Sapi, A. Kukovecz, Z. Konya, H. Jantunen, J. P. Mikkola, and K. Kordas, Phys. Status Solidi B **248**, 2508 (2011).
19) A. Modi, N. Koratkar, E. Lass, B. Q. Wei, and P. M. Ajayan, Nature **424**, 171 (2003).
20) H. Huang, C. H. Liu, and Y. Wu, Adv. Mater. **17**, 1652 (2005).
21) Z. E. Zhen and Y. Ji, J. Zhejiang Univ. **50**, 1671 (2016).
22) T. Borca-Tasciuc, M. Mazumder, Y. Son, S. K. Pal, L. S. Schadler, and P. Ajayan, Nanosci. Nanotechnol. **7**, 1581 (2007).
23) Q. Q. Kong et al., Adv. Funct. Mater. **24**, 4222 (2014).
24) A. K. Geim and K. S. Novoselov, Nat. Mater. **6**, 183 (2007).
25) A. A. Balandin, S. Ghosh, and W. Bao, Nano Lett. **8**, 902 (2008).
26) J. H. Seol et al., Science **328**, 213 (2010).
27) M. Meyyappan, L. Delzeit, A. Cassell, and D. Hash, Plasma Source Sci. T **12**, 205 (2003).
28) A. M. Rao, A. Jorio, M. A. Pimenta, M. S. S. Dantas, R. Saito, and G. Dresselhaus, Phys. Rev. Lett. **84**, 1820 (2000).
29) R. A. Dileo, B. J. Landi, and R. P. Raffaelle, J. Appl. Phys. **101**, 64307 (2007).
30) A. A. Balandin, Nat. Mater. **10**, 569 (2011).